Structural Engineering and Mechanics, Vol. 14, No. 5 (2002) 611-624
DOI: http://dx.doi.org/10.12989/sem.2002.14.5.611

Dynamic plastic response of a hinged-free beam subjected to impact at an arbitrary location along its span

Y. Zhang† and J.L. Yang‡

Solid Mechanics Research Center, Beijing University of Aeronautics and Astronautics, Beijing 100083, P.R. China

Y.L. Hua‡†

Mechanics of Materials Group, China Agricultural University (East Campus), Beijing 100083, P.R. China

(Received June 4, 2002, Accepted September 23, 2002)

Abstract. In this paper, a complete solution is presented for dynamic plastic response of a rigid, perfectly plastic hinged-free beam, of which one end is simply supported or hinged and the other end free, subjected to a transverse strike by a travelling mass at an arbitrary location along its span. The governing differential equations are expressed in non-dimensional forms and solved numerically to obtain the instantaneous deflection of the beam and the plastic dissipated energy in the beam. The dynamic behavior for a hinged-free beam is more complicated than that of a free-free beam. It transpires that the mass ratio and impact position have significant influence on the final deformation. In the aspect of energy dissipation, unlike simply supported or clamped beams for which the plastic deformation consumes almost the total input energy, a considerable portion of the input energy would be transferred as rigid-body motion of hinged-free beam, and the energy dissipated in its plastic deformation is greatly reduced.

Key words: hinged-free beam; dynamic plastic response; impact; plastic dissipated energy.

1. Introduction

The problems of elastoplastic structures subjected to dynamic loading are very complicated because it needs to consider both elastic and plastic deformation, strain-hardening, strain-rate of the materials, and geometrical changes due to large deformation, etc. To avoid the complexity, the rigid, perfectly plastic material model and the assumption of small deformation have been widely adopted to study the dynamic behavior of structures subjected to intense dynamic loading. The rigid, perfectly plastic material idealization is applicable for the structural impact problem if the input energy is much larger than the maximum elastic energy that can be stored in the structure and the

† Ph.D
‡ Professor, Director
‡† Professor

applied pulse was shorter than the fundamental period of the elastic vibration of the structure (Symonds 1967, Symonds *et al.* 1988). This idealization significantly simplifies the deformation mechanism of the structure without losing the key features in its dynamic response.

Over the last fifty years, with this idealization many authors have studied the plastic response of beams with different support conditions or more complex geometric configurations under dynamic loading (Jones 1989, Johnson 1972). One of the earliest and elementary works is that of Lee and Symonds (1952) who considered a free-ended beam of finite length subjected to a transverse force. The problem of impact on the tip of a cantilever was first analyzed by Parkes (1955) and subsequently has been studied by many authors. Ezra (1958) studied a uniform simply supported beam dynamically loaded at its midspan by a rigid striker. Liu and Jones (1988) studied a clamped beam struck by a mass at any point on the span. The problems of dynamic response of beams with more complex configurations have been solved later on (Yu *et al.* 1996, Hua *et al.* 1988). More recently, Yang, Yu and Reid (1998) discussed the dynamic behavior of a free-free beam subjected to step-loading at any arbitrary location along the span. They obtained solutions for various combinations of different magnitudes and locations of loads and also discussed the partitioning of the initial energy dissipation rates for some typical situations.

Between the cases of simply supported beam and free-free beam, there is another kind of beam which is simply supported or hinged at one end and free at the other end, and is called hinged-free beam in this paper. The hinged-free beam can often be seen in engineering structures, for example in the research for pipe systems and rotors of helicopters. By reviewing the previous studies, however, it seems that no attempt has so far been made to study the dynamic behavior of the hinged-free beam. In the aspect of energy dissipation, under the same impact conditions the hinged-free beam is unlike simply supported or clamped beams, for which the plastic deformation consumes almost the total input energy. Compared with the latter, the hinged-free beam is somewhat harder to deform because a considerable portion of the input energy may be transferred as its rigid-body motion and the energy dissipated in its plastic deformation is greatly reduced. This characteristic of dynamic behavior for hinged-free beam is similar to that of free-free beam behavior (Yang *et al.* 1998). So the plastic deformation of the hinged-free beam is certainly less than that of simply supported or clamped beams under the same conditions.

Based on the rigid, perfectly plastic model, the dynamic behavior of hinged-free beams subjected to impact by a travelling mass is studied in this paper. To be more general, the impact position may locate at an arbitrary location along the span of the hinged-free beam. By using the concept of multi-hinge mechanism (Hua *et al.* 1988), the complete solution for the structural response can be obtained from a series of dynamically admissible deformation mechanisms of the structure. All of them not only satisfy the equations of motion, the initial conditions, and boundary conditions, but also do not violate the yield criterion at any point in the structure. Special concern has been paid to study the partitioning of the input energy. The basic assumptions adopted in this paper are:

(1) The material of the beam is rigid, perfectly plastic and rate independent, so that the dynamic fully plastic bending moment $\boldsymbol{M}_p$ is constant.
(2) The beam has uniform cross section and density, and the cross-section possesses an axis of symmetry parallel to the direction of the load.
(3) The effect of the shear force is neglected in the yield condition.
(4) The impact projectile is rigid, and remains in contact with the beam during response process.
(5) The deflection of the beam is small, so that the formulation of the equations of the motion is based on the original configuration.

2. Analysis

As shown in Fig. 1, a hinged-free beam, with length l and mass per unit length of beam m, is subjected to impact by a moving rigid mass at any point on the span. At the instant of impact, i.e., $t = 0$, the rigid mass G strikes on the beam at point A, with speed v_0 in the direction normal to the axe of the beam. It is assumed that after impact the mass remains attached to the beam during the entire response process. Depending on the impact position A, there are different response processes for the hinged-free beam. Each of them consists of three phases. In the following sections, all of them will be discussed in detail.

2.1 Phase 1: $\tau_0 \le \tau \le \tau_1$ (three-hinge mechanism)

Here τ is dimensionless time, which defined in the seventh term of Eq. (3). In Phase 1, there is a stationary hinge at the impact point A, while two travelling plastic hinges, H_1 and H_2, move away from A, see Fig. 2. The velocity diagram is also shown in Fig. 2, in which $\dot{\phi}_1$, $\dot{\theta}_1$, $\dot{\theta}_2$ and $\dot{\phi}_2$ are the absolute angular velocities of segments BH_1, H_1A, AH_2 and H_2C, respectively. $\dot{u}$ and $\dot{y}$ denote the upward velocities of the impact point A and the point at distance x from B, respectively. Using d'Alembert's principle and with some general steps discribed by Hua *et al.* (1988), the equations of for segments BH_1, H_1A, AH_2 and H_2C are derived following

$$m(l_a - x_{h1})^3 \ddot{\phi}_1 = 3M_p \tag{1.1}$$

$$m(l_b - x_{h2})^3 \ddot{\phi}_2 = 12M_p \tag{1.2}$$

$$3mx_{h1}^2 \ddot{u} - 2mx_{h1}^3 \ddot{\theta}_1 = 12M_p \tag{1.3}$$

$$3mx_{h2}^2 \ddot{u} - 2mx_{h2}^3 \ddot{\theta}_2 = 12M_p \tag{1.4}$$

$$\ddot{u} - x_{h1}\ddot{\theta}_1 - (l_a - x_{h1})\ddot{\phi}_1 - \dot{x}_{h1}(\dot{\theta}_1 - \dot{\phi}_1) = 0 \tag{1.5}$$

$$\ddot{u} - x_{h2}\ddot{\theta}_1 - \frac{1}{2}(l_b - x_{h2})\ddot{\phi}_2 - \dot{x}_{h2}(\dot{\theta}_2 - \dot{\phi}_2) = 0 \tag{1.6}$$

$$2m(x_{h1} + x_{h2} + G)\ddot{u} - mx_{h1}^2 \ddot{\theta}_1 - mx_{h2}^2 \ddot{\theta}_2 = 0 \tag{1.7}$$

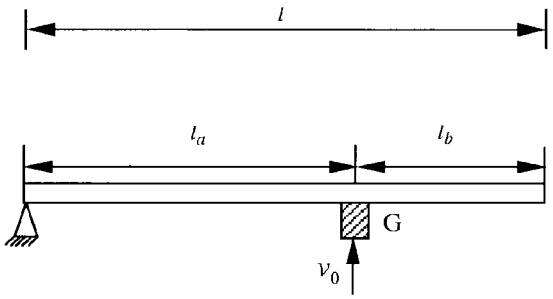

Fig. 1 A hinged-free beam subjected to impact by a projectile

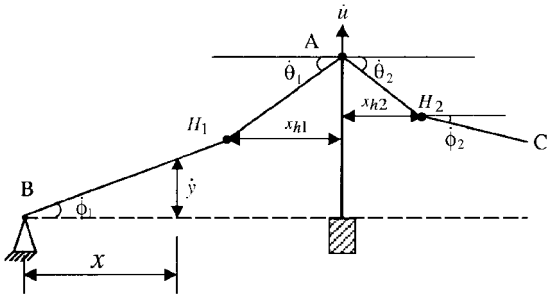

Fig. 2 Velocity diagram for Mechanism ($H_1 - A - H_2$) in Phase 1

And the velocity field is as follows,

$$\dot{y} = \begin{cases} x\dot{\phi}_1 & 0 \le x \le l_a - x_{h1} \\ \dot{u} - (l_a - x)\dot{\theta}_1 & l_a - x_{h1} < x \le l_a \\ \dot{u} - (x - l_a)\dot{\theta}_2 & l_a < x \le l_a + x_{h2} \\ \dot{u} - x_{h2}\dot{\theta}_2 - (x - l_a - x_{h2})\dot{\phi}_2 & l_a + x_{h2} < x \le l \end{cases} \tag{2}$$

For convenience, following dimensionless variables are introduced,

$$\begin{cases} \xi_1 = \dfrac{x_{h1}}{l},\ \xi_2 = \dfrac{x_{h2}}{l},\ \tilde{u} = \dfrac{u}{l},\ \bar{y} = \dfrac{y}{l},\ \bar{x} = \dfrac{x}{l},\ g = \dfrac{G}{ml},\ \tau = t\sqrt{\dfrac{M_p}{ml^3}},\ \eta_1 = \dfrac{l_a}{l},\ \eta_2 = \dfrac{l_b}{l} \\ (\dot{\ }) = \dfrac{d}{dt}(\ ),\ (\ddot{\ }) = \dfrac{d^2}{dt^2}(\ ),\ (\,^{\circ}) = \dfrac{d}{d\tau}(\ ),\ (\,^{\circ\circ}) = \dfrac{d^2}{d\tau^2}(\ ),\ \Lambda = \dfrac{Gv_0^2}{2M_p},\ \hat{E}_p = \dfrac{E_p}{M_p} \end{cases} \tag{3}$$

where l_a, l_b, x_{h1}, and x_{h2} denote the lengths of AB, AC, H_1A and AH_2, respectively, and E_p denotes the plastic dissipation energy.

Then Eqs. (1) and (2) can be non-dimensionalized as

$$\overset{\circ\circ}{\phi}_1 = \frac{3}{(\eta_1 - \xi_1)^3} \tag{4.1}$$

$$\overset{\circ\circ}{\phi}_2 = \frac{12}{(\eta_2 - \xi_2)^3} \tag{4.2}$$

$$\overset{\circ\circ}{\tilde{u}} = -\frac{12(\xi_1 + \xi_2)}{\xi_1\xi_2(\xi_1 + \xi_2 + 4g)} \tag{4.3}$$

$$\overset{\circ\circ}{\theta}_1 = -\frac{18(\xi_1 + \xi_2)}{\xi_1^2\xi_2(\xi_1 + \xi_2 + 4g)} - \frac{6}{\xi_1^3} \tag{4.4}$$

$$\overset{\circ\circ}{\theta}_2 = -\frac{18(\xi_1 + \xi_2)}{\xi_1\xi_2^2(\xi_1 + \xi_2 + 4g)} - \frac{6}{\xi_2^3} \tag{4.5}$$

$$\overset{\circ}{\xi}_1(\overset{\circ}{\theta}_1 - \overset{\circ}{\phi}_1) = \frac{6(\xi_1 + \xi_2)}{\xi_1\xi_2(\xi_1 + \xi_2 + 4g)} + \frac{6}{\xi_1^2} - \frac{3}{(\eta_1 - \xi_1)^2} \tag{4.6}$$

$$\overset{\circ}{\xi}_2(\overset{\circ}{\theta}_2 - \overset{\circ}{\phi}_2) = \frac{6(\xi_1 + \xi_2)}{\xi_1\xi_2(\xi_1 + \xi_2 + 4g)} + \frac{6}{\xi_2^2} - \frac{6}{(\eta_2 - \xi_2)^2} \tag{4.7}$$

and

$$\dot{\bar{y}} = \begin{cases} \bar{x}\dot{\phi}_1 & 0 \le \bar{x} \le \eta_1 - \xi_1 \\ \dot{\tilde{u}} - (\eta_1 - \bar{x})\dot{\theta}_1 & \eta_1 - \xi_1 < \bar{x} \le \eta_1 \\ \dot{\tilde{u}} - (\bar{x} - \eta_1)\dot{\theta}_2 & \eta_1 < \bar{x} \le \eta_1 + \xi_2 \\ \dot{\tilde{u}} - \xi_2\dot{\theta}_2 - (\bar{x} - \eta_1 - \xi_2)\dot{\phi}_2 & \eta_1 + \xi_2 < \bar{x} \le 1 \end{cases} \tag{5}$$

For the typical case that the rigid mass strikes at the free end of the hinged-free beam, i.e., $\eta_1 = 1$, the non-dimensional governing equations and velocity field of the beam are found to be

$$\ddot{\tilde{u}} = -\frac{6}{\xi(\xi + 4g)} \tag{4'.1}$$

$$\ddot{\theta}_1 = -\frac{12(\xi + g)}{\xi^3(\xi + 4g)} \tag{4'.2}$$

$$\ddot{\phi}_1 = \frac{3}{(1 - \xi)^3} \tag{4'.3}$$

$$\dot{\xi}(\dot{\theta}_1 - \dot{\phi}_1) = -\frac{6}{\xi(\xi + 4g)} + \frac{12(\xi + g)}{\xi^2(\xi + 4g)} - \frac{3}{(1 - \xi)^2} \tag{4'.4}$$

and

$$\dot{\bar{y}} = \begin{cases} \bar{x}\dot{\phi}_1 & 0 \le \bar{x} \le 1 - \xi \\ \dot{u} - (1 - \bar{x})\dot{\theta}_1 & 1 - \xi < \bar{x} \le 1 \end{cases} \tag{5}$$

With appropriate initial conditions, Eqs. (4) and (5) can be solved by using a Runge-Kutta procedure. When $\tau = 0$, we have $\xi_1 = 0$, $\xi_2 = 0$, $\dot{\xi}_1 \to \infty$, and $\dot{\xi}_2 \to \infty$ from Eqs. (4) and (5). Therefore the initial conditions at $\tau = 0$ are inappropriate for numerical calculations. Employing conditions at an infinitesimal time τ_0 replacing that at $\tau = 0$ may solve this difficulty.

From Eq. (4) it could be found that for a small interval of time after impact, $\ddot{\phi}_1$ and $\ddot{\phi}_2$ are finite and negligible in comparison with $\ddot{\tilde{u}}$, $\dot{\xi}_1$ and $\dot{\xi}_2$. For the same reason $\dot{\phi}_1$, $\dot{\phi}_2$ can be neglected. Furthermore, when $\tau = \tau_0$ we have $\xi_1 = \xi_2$ approximately. According to the velocity continuous condition at travelling hinge H_1, we have

$$(\eta_1 - \xi_1)\dot{\phi}_1 = \dot{\tilde{u}} - \xi_1\dot{\theta}_1 \tag{6}$$

Eq. (6) yields

$$\dot{\theta}_1 = \frac{\dot{\tilde{u}}}{\xi_1} \tag{7}$$

Differentiating Eq. (6) with respect to τ gives

$$\ddot{\theta}_1 = \frac{\xi_1\ddot{\tilde{u}} - \xi_1(\eta_1 - \xi_1)\ddot{\phi}_1 + \dot{\xi}_1(\eta_1\dot{\phi}_1 - \dot{\tilde{u}})}{\xi_1^2} \tag{8}$$

Substituting $\xi_1 = \xi_2$ and Eq. (8) into Eqs. (4.3) and (4.4), the two differential equations can be reduced to the following approximate equation in dimensionless form

$$(\xi_1 + g)\overset{\circ\circ}{\tilde{u}} + \overset{\circ}{\xi}_1\overset{\circ}{\tilde{u}} = 0 \tag{9}$$

$$\xi_1^2\overset{\circ\circ}{\tilde{u}} + 2\xi_1\overset{\circ}{\xi}_1\overset{\circ}{\tilde{u}} = 12 \tag{10}$$

Eqs. (9) and (10) can be rewritten as

$$d((g + \xi_1)\overset{\circ}{\tilde{u}})/d\tau = 0 \tag{11}$$

$$d(\xi_1^2\overset{\circ}{\tilde{u}})/d\tau = 12 \tag{12}$$

Integrating Eqs. (11) and (12) and using the initial conditions $\tau = 0$, $\xi_1 = 0$ and $\overset{\circ}{\tilde{u}} = \sqrt{2\Lambda/g}$, lead to

$$\tau_0 = \frac{\xi_1^2 g\sqrt{2\Lambda/g}}{12(\xi_1 + g)} \tag{13}$$

$$\overset{\circ}{\tilde{u}} = \frac{g\sqrt{2\Lambda/g}}{\xi_1 + g} \tag{14}$$

From Eqs. (7) and (14), it yields:

$$\overset{\circ}{\theta}_1 = \frac{g\sqrt{2\Lambda/g}}{\xi_1(\xi_1 + g)} \tag{15}$$

The values of τ_0 and $\overset{\circ}{\tilde{u}}$ can be determined as long as an arbitrarily small value of ξ_1 is chosen. The other variables are small enough to be considered as zero. When a small ξ_1 is given, we can get the initial conditions as follows

$$\tau = \tau_0 = \frac{\xi_1^2 g\sqrt{2\Lambda/g}}{12(\xi_1 + g)},\ \tilde{u} = 0,\ \overset{\circ}{\tilde{u}} = \frac{g\sqrt{2\Lambda/g}}{\xi_1 + g},\ \theta_1 = \theta_2 = 0,\ \overset{\circ}{\theta}_1 = \overset{\circ}{\theta}_2 = \frac{g\sqrt{2\Lambda/g}}{\xi_1(\xi_1 + g)}$$

$$\phi_1 = \overset{\circ}{\phi}_1 = 0,\ \phi_2 = \overset{\circ}{\phi}_2 = 0,\ \xi_2 = \xi_1 \tag{16}$$

and

$$\bar{y} = 0 \qquad 0 \le \bar{x} \le 1 \tag{17}$$

For the typical case that the rigid mass strike at the free end of the hinged-free beam, the initial conditions can be expressed as

$$\tau = \tau_0 = \frac{\xi^2 g\sqrt{2\Lambda/g}}{3(\xi + 2g)},\ \tilde{u} = 0,\ \overset{\circ}{\tilde{u}} = \frac{2g\sqrt{2\Lambda/g}}{\xi + 2g},\ \theta_1 = 0,\ \overset{\circ}{\theta}_1 = \frac{2g\sqrt{2\Lambda/g}}{\xi(\xi + 2g)},\ \phi_1 = \overset{\circ}{\phi}_1 = 0 \tag{16'}$$

and

$$\bar{y} = 0 \qquad 0 \le \bar{x} \le 1 \tag{17'}$$

Non-linear ordinary differential Eqs. (4) and (5) with initial conditions (16) and (17) can be solved numerically.

For case of $\eta_1 < 1$, Phase 1 terminates either when the left travelling hinge H_1 vanishes, i.e., $\mathring{\theta}_1 - \mathring{\phi}_1 = 0$, or when the right travelling hinge H_2 vanishes, i.e., $\mathring{\theta}_2 - \mathring{\phi}_2 = 0$ at $\tau = \tau_1$. But for $\eta_1 = 1$, Phase 1 terminates only when $\mathring{\theta}_1 - \mathring{\phi}_1 = 0$ at $\tau = \tau_1$.

Now discussing the energy dissipated in the plastic hinges during Phase 1.

(1) Phase 1 terminates when H_1 vanishes first. The plastic dissipated energy $\hat{E}_{p1}$ in Phase 1 equals to the initial kinetic energy minus the kinetic energy of the beam, and can be expressed in a non-dimensional form as

$$\hat{E}_{p1} = \Lambda - \frac{1}{6}[3(\eta_1 + \eta_2 + g)\mathring{\tilde{u}}^{(1)2} + \eta_1^3\mathring{\theta}_1^{(1)2} + (3\eta_2 - 2\xi_2^{(1)})\mathring{\theta}_2^{(1)2} + (\eta_2 - \xi_2^{(1)})^3\mathring{\phi}_1^{(1)2}$$
$$- 3\eta_1^2\mathring{\tilde{u}}^{(1)}\mathring{\theta}_1^{(1)} + 3\xi_2^{(1)}(\xi_2^{(1)} - 2\eta_2)\mathring{\tilde{u}}^{(1)}\mathring{\theta}_2^{(1)} - 3(\eta_2 - \xi_2^{(1)})^2(\mathring{\tilde{u}}^{(1)} - \xi_2^{(1)}\mathring{\theta}_2^{(1)})\,\mathring{\phi}_2^{(1)2}] \tag{18}$$

where $\mathring{\tilde{u}}^{(1)}, \mathring{\theta}_1^{(1)}, \mathring{\theta}_2^{(1)}, \mathring{\phi}_1^{(1)}, \mathring{\phi}_2^{(1)}, \xi_1^{(1)}$ and $\xi_2^{(1)}$ are the corresponding values of $\mathring{\tilde{u}}, \mathring{\theta}_1, \mathring{\theta}_2, \mathring{\phi}_1, \mathring{\phi}_2, \xi_1$ and ξ_2 at the end of Phase 1.

For $\eta_1 = 1$, the Eq. (18) can be simplified as

$$\hat{E}_p = \Lambda - \frac{1}{6}(1 + 3g)\mathring{\tilde{u}}^{(1)2} \tag{18'}$$

(2) Phase 1 terminates when H_2 vanishes first. The dimensionless plastic dissipated energy $\hat{E}_{p1}$ in Phase 1 is

$$\hat{E}_{p1} = \Lambda - \frac{1}{6}[3(\xi_1^{(1)} + \eta_2 + g)\mathring{\tilde{u}}^{(1)2} + \xi_1^{(1)3}\mathring{\theta}_1^{(1)2} + \eta_2^3\mathring{\theta}_2^{(1)2} + (\eta_1 - \xi_1^{(1)})^3\mathring{\phi}_1^{(1)2}$$
$$-3\xi_1^{(1)2}\mathring{\tilde{u}}^{(1)}\mathring{\theta}_1^{(1)} - 3\eta_2^2\mathring{\tilde{u}}^{(1)}\mathring{\theta}_2^{(1)}] \tag{19}$$

For the case of impact position at free-end of the beam, i.e., $\eta_1 = 1$, the beam rotates about B as a rigid body after Phase 1 terminates, and it will not be discussed further.

2.2 Phase 2: $\tau_1 \le \tau \le \tau_2$ (two-hinge mechanism)

The following discussions are only for cases of $\eta_1 < 1$.

(1) Mechanism ($A - H_2$). If H_1 vanishes first, the deformation mechanism of the beam consists of a stationary hinge A and a travelling hinge H_2 in Phase 2. For this mechanism the velocity diagram is shown in Fig. 3, in which $\dot{u}, \dot{\theta}_2, \dot{\phi}_2, x_{h2}, \dot{y}$ and x denote the same variables as those in Phase 1. By means of a procedure similar to that in Phase 1, the non-dimensional governing equations and velocity field are given by

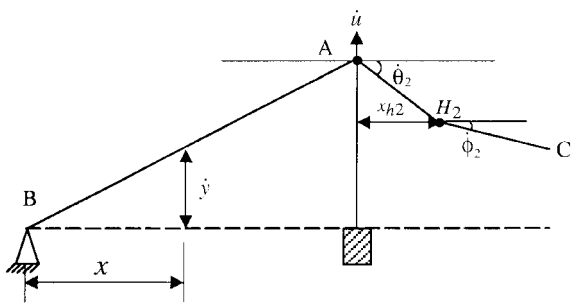

Fig. 3 Velocity diagram for Mechanism ($A - H_2$) in Phase 2

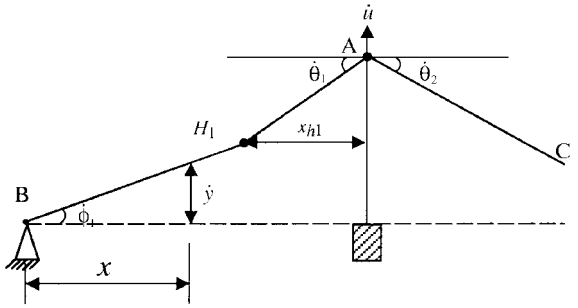

Fig. 4 Velocity diagram for Mechanism ($H_1 - A$) in Phase 2

$$\overset{\circ\circ}{\phi}_2 = \frac{12}{(\eta_2 - \xi_2)^3} \tag{20.1}$$

$$\overset{\circ\circ}{\tilde{u}} = -\frac{12(3\eta_1 + \xi_2)}{\eta_1\xi_2(4\eta_1 + 3\xi_2 + 12g)} \tag{20.2}$$

$$\overset{\circ\circ}{\theta}_2 = -\frac{18(3\eta_1 + \xi_2)}{\eta_1\xi_2^2(4\eta_1 + 3\xi_2 + 12g)} - \frac{6}{\xi_2^3} \tag{20.3}$$

$$\overset{\circ}{\xi}_2(\overset{\circ}{\theta}_2 - \overset{\circ}{\phi}_2) = \frac{6(3\eta_1 + \xi_2)}{\eta_1\xi_2(4\eta_1 + 3\xi_2 + 12g)} + \frac{6}{\xi_2^2} - \frac{6}{(\eta_2 - \xi_2)^2} \tag{20.4}$$

and

$$\overset{\circ}{\bar{y}} = \begin{cases} \bar{x}\overset{\circ}{\tilde{u}} / \eta_1 & 0 \le \bar{x} \le \eta_1 \\ \overset{\circ}{\tilde{u}} - (\bar{x} - \eta_1)\overset{\circ}{\theta}_2 & \eta_1 < \bar{x} \le \eta_1 + \xi_2 \\ \overset{\circ}{\tilde{u}} - \xi_2\overset{\circ}{\theta}_2 - (\bar{x} - \eta_1 - \xi_2)\overset{\circ}{\phi}_2 & \eta_1 + \xi_2 < \bar{x} \le 1 \end{cases} \tag{21}$$

The initial conditions of Phase 2 are derived from the instant state when Phase 1 terminates. This deformation mechanism is valid until $\overset{\circ}{\theta}_2 - \overset{\circ}{\phi}_2 = 0$ when the right hinge H_2 vanishes at $\tau = \tau_2$. The non-dimensional plastic dissipated energy in Phase 2 is given by

$$\hat{E}_{p2} = \Lambda - \hat{E}_{p1} - \frac{1}{6}[(\eta_1 + 3\eta_2 + 3g)\overset{\circ}{\tilde{u}}^{(2)^2} + \eta_2^3\overset{\circ}{\theta}_2^{(2)^2} - 3\eta_2^2\overset{\circ}{\tilde{u}}^{(2)}\overset{\circ}{\theta}_2^{(2)}] \tag{22}$$

where $\overset{\circ}{\tilde{u}}^{(2)}, \overset{\circ}{\theta}_2^{(2)}, \overset{\circ}{\phi}_2^{(2)}$ and $\xi_2^{(2)}$ are the corresponding values of $\overset{\circ}{\tilde{u}}$, $\overset{\circ}{\theta}_2$, $\overset{\circ}{\phi}_2$ and ξ_2 at the end of Phase 2, respectively.

(2) Mechanism ($H_1 - $A). If hinge H_2 vanishes first, the deformation mechanism of the beam consists of a travelling hinge H_1 and a stationary hinge A in Phase 2. For this deformation mechanism the velocity diagram is shown in Fig. 4. The non-dimensional governing equations and velocity field can be expressed as

$$\overset{\circ\circ}{\phi}_1 = \frac{3}{(\eta_1 - \xi_1)^3} \tag{23.1}$$

$$\overset{\circ\circ}{\tilde{u}} = -\frac{6(\xi_1 + 2\eta_2)}{\xi_1\eta_2(\xi_1 + \eta_2 + 4g)} \tag{23.2}$$

$$\overset{\circ\circ}{\theta}_1 = -\frac{9(\xi_1 + 2\eta_2)}{\xi_1^2\eta_2(\xi_1 + \eta_2 + 4g)} - \frac{6}{\xi_1^3} \tag{23.3}$$

$$\overset{\circ\circ}{\theta}_2 = -\frac{9(\xi_1 + 2\eta_2)}{\xi_1\eta_2^2(\xi_1 + \eta_2 + 4g)} - \frac{3}{\eta_2^3} \tag{23.4}$$

$$\overset{\circ}{\xi}_1(\overset{\circ}{\theta}_1 - \overset{\circ}{\phi}_1) = \frac{3(\xi_1 + 2\eta_2)}{\xi_1\eta_2(\xi_1 + \eta_2 + 4g)} + \frac{6}{\xi_1^2} - \frac{3}{(\eta_1 - \xi_1)^2} \tag{23.5}$$

and

$$\overset{\circ}{\bar{y}} = \begin{cases} \bar{x}\,\overset{\circ}{\phi}_1 & 0 \le \bar{x} \le \eta_1 - \xi_1 \\ \overset{\circ}{\tilde{u}} - (\eta_1 - \bar{x})\overset{\circ}{\theta}_1 & \eta_1 - \xi_1 < \bar{x} \le \eta_1 \\ \overset{\circ}{\tilde{u}} - (\bar{x} - \eta_1)\overset{\circ}{\theta}_2 & \eta_1 < \bar{x} \le 1 \end{cases} \tag{24}$$

The initial conditions for Phase 2 are obtained from the instant state when Phase 1 terminates. This deformation mechanism is valid until either $\overset{\circ}{\theta}_1 - \overset{\circ}{\phi}_1 = 0$ or $\overset{\circ}{\theta}_1 + \overset{\circ}{\theta}_2 = 0$ at $\tau = \tau_2$, i.e., when the left hinge H_1 vanishes or when the stationary hinge A becomes inactive. Accordingly the non-dimensional plastic dissipated energy $\hat{E}_{p2}$ in Phase 2 can be found as follows.

(1) Corresponding to $\overset{\circ}{\theta}_1 - \overset{\circ}{\phi}_1 = 0$ at the end of Phase 2

$$\hat{E}_{p2} = \Lambda - \hat{E}_{p1} - \frac{1}{6}[(\eta_1 + 3\eta_2 + 3g)\overset{\circ}{\tilde{u}}^{(2)^2} + \eta_2^3\overset{\circ}{\theta}_2^{(2)^2} - 3\eta_2^2\overset{\circ}{\tilde{u}}^{(2)}\overset{\circ}{\theta}_2^{(2)}] \tag{25}$$

(2) Corresponding to $\overset{\circ}{\theta}_1 + \overset{\circ}{\theta}_2 = 0$ at the end of Phase 2

$$\hat{E}_{p2} = \Lambda - \hat{E}_{p1} - \frac{1}{6}[3(\xi_1^{(2)} + \eta_2 + g)\overset{\circ}{\tilde{u}}^{(2)^2} + \xi_1^{(2)^3}\overset{\circ}{\theta}_1^{(2)^2} + (\eta_1 - \xi_1^{(2)})^3\overset{\circ}{\phi}_1^{(1)^2} - 3\xi_1^{(2)^2}\overset{\circ}{\tilde{u}}^{(2)}\,\overset{\circ}{\theta}_1^{(2)}] \tag{25'}$$

where $\overset{\circ}{\tilde{u}}^{(2)}$, $\overset{\circ}{\theta}_1^{(2)}$, $\overset{\circ}{\theta}_2^{(2)}$ and $\xi_1^{(2)}$ are the values of $\overset{\circ}{\tilde{u}}$, $\overset{\circ}{\theta}_1$, $\overset{\circ}{\theta}_2$ and ξ_1 at the end of Phase 2, respectively.

2.3 Phase 3: $\tau_2 \le \tau \le \tau_3$ (single-hinge mechanism)

(1) Mechanism (A). This deformation mechanism consists of a stationary hinge A only, and its velocity diagram is shown in Fig. 5. By similar analysis adopted above the non-dimensional governing equations and velocity field can be obtained as follows

$$\overset{\circ\circ}{\tilde{u}} = -\frac{6(3\eta_1 + 2\eta_2)}{\eta_1\eta_2(4\eta_1 + 3\eta_2 + 12g)} \tag{26.1}$$

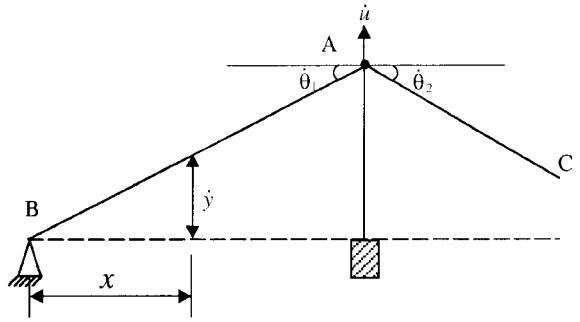

Fig. 5 Velocity diagram for mechanism (*A*) in Phase 3

$$\overset{\circ\circ}{\theta}_2 = -\frac{9(3\eta_1 + 2\eta_2)}{\eta_1\eta_2^2(4\eta_1 + 3\eta_2 + 12g)} - \frac{3}{\eta_2^3} \tag{26.2}$$

and

$$\overset{\circ}{\bar{y}} = \begin{cases} \bar{x}\overset{\circ}{\bar{u}} / \eta_1 & 0 \le \bar{x} \le \eta_1 \\ \overset{\circ}{\bar{u}} - (\bar{x} - \eta_1)\overset{\circ}{\theta}_2 & \eta_1 < \bar{x} \le 1 \end{cases} \tag{27}$$

The initial conditions for Phase 3 can be obtained from the instant state when Phase 2 terminates. When $\overset{\circ}{\theta}_1 + \overset{\circ}{\theta}_2 = 0$ at $\tau = \tau_3$, Phase 3 terminates. The non-dimensional plastic dissipated energy $\hat{E}_{p3}$ in Phase 3 is

$$\hat{E}_{p3} = \Lambda - \hat{E}_{p1} - \hat{E}_{p2} - \frac{1}{6}(\eta_1 + 3\eta_2 + 3g)\overset{\circ}{\tilde{u}}^{(3)^2} \tag{28}$$

where $\overset{\circ}{\tilde{u}}^{(3)}$ is the non-dimensional upward velocity of the impact point at the end of Phase 3. Then for this case the total non-dimensional plastic dissipated energy during the response process can be calculated from

$$\hat{E}_p = \Lambda - \frac{1}{6}(\eta_1 + 3\eta_2 + 3g)\overset{\circ}{\tilde{u}}^{(3)^2} \tag{29}$$

(2) Mechanism (H_1). This mechanism consists of a travelling hinge H_1 only. For this case the segment H_1C rotates about the travelling hinge H_1 and the velocity diagram is shown in Fig. 6. By

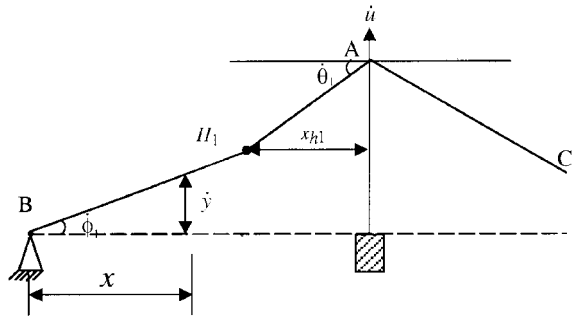

Fig. 6 Velocity diagram for mechanism (H_1) in Phase 3

similar analysis the non-dimensional governing equations and velocity field can be obtained as follows

$$\overset{\circ\circ}{\phi}_1 = \frac{3}{(1-\xi_1)^3} \tag{30.1}$$

$$\overset{\circ\circ}{\tilde{u}} = -\frac{18(\xi_1+\eta_2)}{\eta_2^3+5\eta_2^2\xi_1+5\eta_2\xi_1^2+\xi_1^3+4g(\eta_2^2+\eta_2\xi_1+\xi_1^2)} \tag{30.2}$$

$$\overset{\circ\circ}{\theta}_1 = -\frac{36(\xi_1+\eta_2+8)}{\eta_2^4+4\eta_2^3\xi_1-4\eta_2\xi_1^3-\xi_1^4+4g(\eta_2^3-\xi_1^3)} \tag{30.3}$$

$$\overset{\circ}{\xi}_1(\overset{\circ}{\theta}_1-\overset{\circ}{\phi}_1) = \overset{\circ\circ}{\tilde{u}}-\xi_1\overset{\circ\circ}{\theta}_1 - \frac{3}{(1-\xi_1)^2} \tag{30.4}$$

and

$$\overset{\circ}{\bar{y}} = \begin{cases} \bar{x}\overset{\circ}{\phi}_1 & 0 \le \bar{x} \le \eta_1-\xi_1 \\ \overset{\circ}{\tilde{u}} - (\eta_1-\bar{x})\overset{\circ}{\theta}_1 & \eta_1-\xi_1 < \bar{x} \le \eta_1 \\ \overset{\circ}{\tilde{u}} + (\bar{x}-\eta_1)\overset{\circ}{\theta}_1 & \eta_1 < \bar{x} \le 1 \end{cases} \tag{31}$$

The initial conditions of Phase 3 are derived from the instant state when Phase 2 terminates. When $\overset{\circ}{\theta}_1-\overset{\circ}{\phi}_1 = 0$ at $\tau = \tau_3$, Phase 3 terminates, i.e., the travelling hinge H_1 vanishes. The non-dimensional plastic dissipated energy $\hat{E}_{p3}$ in Phase 3 is

$$\hat{E}_{p3} = \Lambda - \hat{E}_{p1} - \hat{E}_{p2} - \frac{1}{6}\left(\frac{1}{\eta_1^2}+3g\right)\overset{\circ}{\tilde{u}}^{(3)2} \tag{32}$$

where $\overset{\circ}{\tilde{u}}^{(3)}$ is the non-dimensional upward velocity of the impact point at the end of Phase 3. Then for this case the total non-dimensional plastic dissipated energy during the response process can be calculated from

$$\hat{E}_p = \Lambda - \frac{1}{6}\left(\frac{1}{\eta_1^2}+3g\right)\overset{\circ}{\tilde{u}}^{(3)2} \tag{33}$$

2.4 Phase 4: $\tau \ge \tau_3$ (rigid-body motion)

In Phase 4, the beam rotates about B as a rigid body, and no more plastic deformation occurs afterwards. Here, it will not be discussed further.

3. Numerical results and discussions

3.1 Numerical results of deflection of the beam and position of hinges

There are three independent variables in this problem, i.e., mass ratio g, input energy Λ and impact position η_1. The numerical solutions for several different combinations of mass ratio and

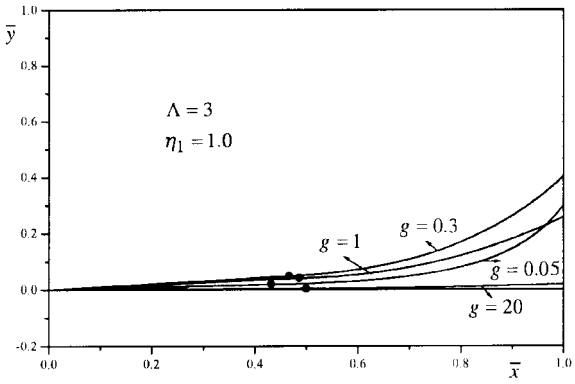

Fig. 7 Final deformed shapes and final positions of moving hinge

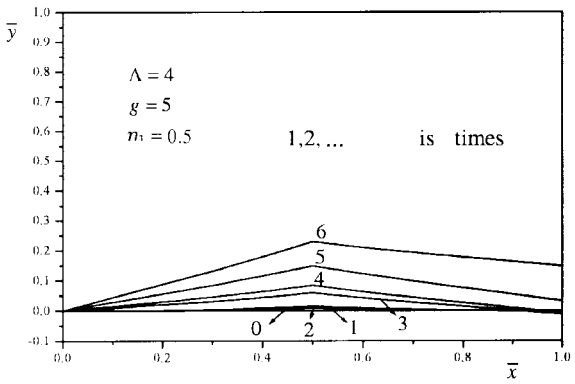

Fig. 8 Instantaneous profile and final deformed shapes

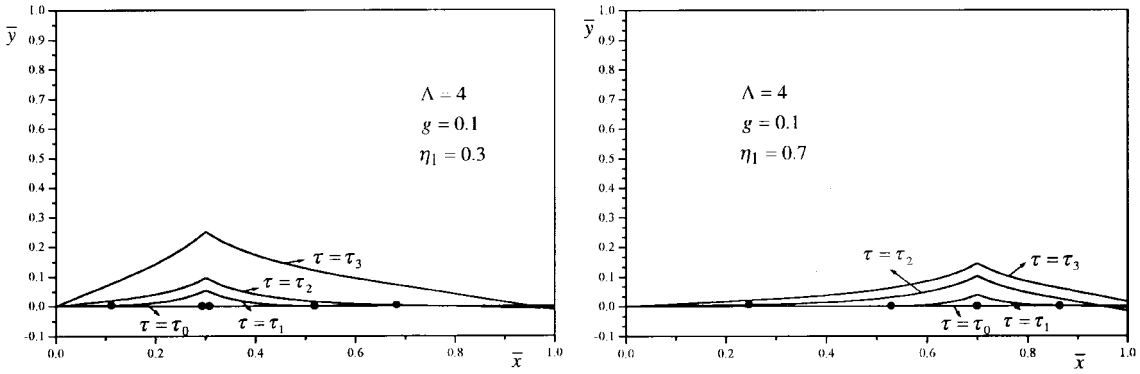

Fig. 9 Final deformed shapes of each phase and positions of moving hinge

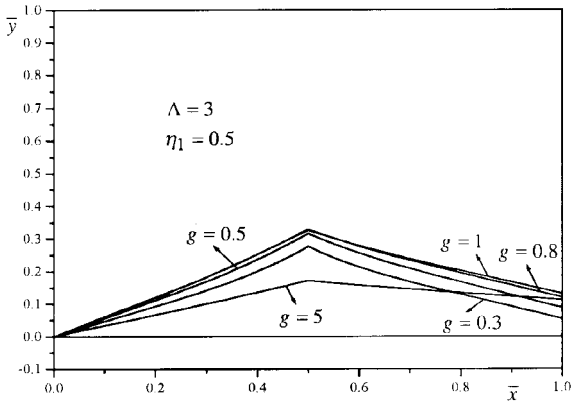

Fig. 10 Curves of final deformation verses mass ratio

input energy are shown in Figs. 7-10 graphically. For η_1 = 1 and Λ = 3 Fig. 7 shows that the final profiles of the deformed beam and final position of the travelling hinge. For given impact situations, Fig. 8 shows the instantaneous profiles of the deformed beam at different instants and Fig. 9 shows

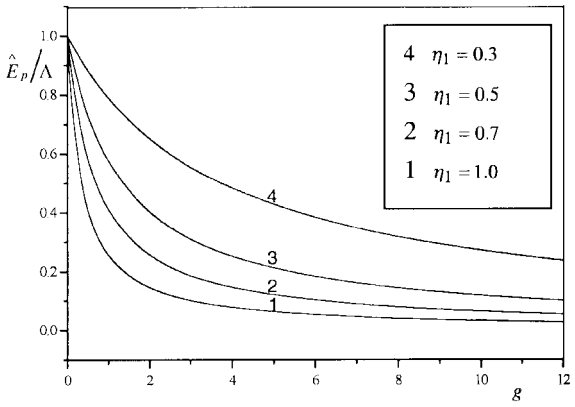

Fig. 11 Curves of dissipated energy verses mass ratio

the instantaneous profiles of the deformed beam at the end of each phase, respectively. When impact position η_1 and input energy Λ are given, the relationship between final profile and mass ratio can be found numerically, and is plotted in Fig. 10 for $\eta_1 = 0.5$ and $\Lambda = 3$. According to the numerical results, following discussions can be made.

(1) When the initial impact energy and impact position are given, the mass ratio will significantly influence the final profile of the beam, the final deflection of the impact point and the response time. There is a critical value of mass ratio for which the final deflection of the impact point is the largest. When $\eta_1 = 0.5$, for example, the critical value of mass ratio approximately equals 0.8 as shown in Fig. 10. Furthermore, the response time does not monotonously vary with mass ratio, and also there exits a critical value of mass ration for which the response time is the longest. When $\eta_1 = 1.0$, for example, the critical value of mass ratio approximately equals 0.3.

(2) Wherever the impact position is, two travelling hinges move away from the impact point after impact and vanish in the vicinity of midsections of the right and left segments of the beam, respectively. For given initial impact energy and impact position, the final positions of two travelling hinges approach to the midsections of the two segments when mass ratio increases, respectively. Furthermore, when given mass ratio and the impact position, the vanishing positions of the traveling hinges are independent of the initial impact energy.

(3) When the mass ratio and the impact position are given, the deflection of the beam increases with the input energy. The deformation mechanism of the beam in Phase 2 and 3 depends on the impact position only, and is independent of the mass ratio and the initial energy.

(4) When the initial impact energy and the mass ratio are given, the impact position greatly influences the response time of each phase.

3.2 Energy dissipation

It is of great interests for engineering applications to discuss the partition of the input energy between kinetic energy of rigid body motion and dissipated energy on the plastic deformation of the beam. The plastic dissipated energy determines the permanent profile and possible failure mode of the beam.

The curves of $\hat{E}/\Lambda$ versus g for given η_1 are shown in Fig. 11. It is observed that when the

impact position is given, the total plastic dissipation work decreases with the increase of mass ratio. When $g < 1$, almost all of the input energy is dissipated on the plastic deformations of the beam during the response process. However, when $g > 5$ no more than 30% and 50% of the input energy are dissipated by plastic deformation for $\eta_1 = 0.5$ and $\eta_1 = 0.7$, respectively. As for $g > 5$ and $\eta_1 = 1.0$, i.e., when the rigid mass strikes the free end of the beam, the plastic dissipation is less than 10% of the input energy, and most of the input energy transforms to the kinetic energy of rigid body motion of the beam.

4. Conclusions

By using a series of dynamically admissible deformation mechanisms of the structure, the response process of a rigid, perfectly plastic hinged-free beam, which struck by a rigid mass at an arbitrary location along its span, is analyzed so that a complete solution for the structural response can be obtained. The present theoretical results expressed in terms of non-dimensional parameters demonstrated that the mass ratio and impact position have significant influence on the final deformation and the plastic dissipated energy in the beam. The response process of hinged-free beam is more complicated than that of free-free beam because of the influence of impact position. In the aspect of energy dissipation, unlike simply supported or clamped beams for which the plastic deformation consumes almost the total input energy, a considerable portion of the input energy would be transferred as rigid-body motion of hinged-free beam and the energy dissipated in its plastic deformation is greatly reduced. Therefore, compared with them, under the same impact conditions, the hinged-free beam is somewhat harder to deform. When the impact position is given, the less the mass ratio is, the more the energy dissipated.

References

Ezra, A.A. (1958), "The plastic response of a simply supported beam to an impact load at its center", *Proc. Third U.S. Nat. Congr. Appl. Mech., Am. Soc. Mech. Engrs*., 513-528.

Hua, Y.L., Yu, T.X. and Reid, S.R. (1988), "Double-hinge modes in the dynamic response of plastic cantilever beams subjected to step loading", *Int. J. Impact Engng.*, **7**, 401-413.

Jones, N. (1989), *Structural Impact*, Cambridge UP, Cambridge.

Johnson, W. (1972), *Impact Strength of Materials*, Edward Arnold, London, and Crane Russak, New York.

Lee, E.H. and Symonds, P.S. (1952), "Large plastic deformation of beams under transverse impact", *J. Appl. Mech.*, **19**, 308-314.

Liu, J.H. and Norman Jones, (1988), "Dynamic response of a rigid plastic clamped beam struck by a mass at any point on the span", *Int. J. Solids Structures*, **24**(3), 251-270.

Parkes, E.W. (1955), "The permanent deformation of a cantilever struck transversely at its tip", *Proc. R. Soc*., Series A, 228-462.

Symonds, P.S. (1967), "Survey of methods of analysis for plastic deformation of structure under dynamic loading", Brown University, Division of Engineering Report BU/NSRDC/1-67.

Symond, P.S. and Frye, C.W.G. (1988), "On the relation between rigid-plastic and elastic-plastic predictions of response to pulse loading", *Int. J. Impact Engng*., **7**, 139-149.

Yang, J.L., Yu, T.X. and Reid, S.R. (1998), "Dynamic behavior of a rigid, perfectly plastic free-free beam subjected to step-loading at an arbitrary location along its span", *Int. J. Impact Engng.*, **21**(3), 165-175.

Yu, T.X., Hua, Y.L. and Reid, S.R. (1996), "Incipient deformation mechanisms of a semi-circular cantilever beam subjected to an out-of-plane step-loading", *Int. J. Impact Engng*., **18**, 829-848.